Supplementary Information for the manuscript: Leaf habit affects the distribution of drought sensitivity but not water transport efficiency in the tropics

German Vargas G.[1,2,*], Norbert Kunert[3,4,5], William M. Hammond[6], Z. Carter Berry[7], Leland K. Weden[8], Chris M. Smith-Martin[9], Brett T. Wolfe[4,10], Laura Toro[1], Ariadna Mondragón-Botero[1], Jesús N. Pinto-Ledezma[11], Naomi B. Schwartz[12], María Uriarte[9], Lawren Sack[13], Kristina J. Anderson-Teixeira[3,4] and Jennifer S. Powers[1,11]

[1]Department of Plant and Microbial Biology, University of Minnesota, St. Paul, MN 55108, USA.
[2]School of Biological Sciences, The University of Utah, Salt Lake City, UT 84112, USA.
[3]Conservation Ecology Center, Smithsonian National Zoo and Conservation Biology Institute, Front Royal, VA 22630, USA.
[4]Forest Global Earth Observatory, Smithsonian Tropical Research Institute, Panama, Republic of Panama.
[5]Department of Integrative Biology and Biodiversity Research, Institute of Botany, University of Natural Resources and Life Sciences Vienna, Vienna A-1190, Austria.
[6]Agronomy Department, Institute of Food and Agricultural Sciences, University of Florida, Gainesville, FL 32611, USA.
[7]Department of Biology, Wake Forest University, Winston-Salem, NC 27109, USA.
[8]Department of Environmental Systems Science, ETH Zürich, Zürich, Switzerland.
[9]Department of Ecology, Evolution and Environmental Biology, Columbia University, New York, NY 10027, USA.
[10]School of Renewable Natural Resources, Louisiana State University Agricultural Center, Baton Rouge, LA 70803, USA.
[11]Department of Ecology, Evolution and Behavior, University of Minnesota, St. Paul, MN 55108, USA.
[12]Department of Geography, University of British Columbia, Vancouver, BC V6T 1Z2, Canada.
[13]Department of Ecology and Evolution, University of California Los Angeles, Los Angeles, CA 90095, USA.
* Correspondence to: german.vargas@utah.edu

Table S1. Correlation matrix table among five climatic predictors: aridity index (AI), dry season length (DSL), maximum climatic water deficit (MCWD), seasonality index (S), and mean annual rainfall (MAR). Values represent the Pearson's product moment correlation coefficient.

Median climatic affiliations:						
		AI	DSL	MCWD	S	MAR
	AI	1.00	-0.78	0.80	-0.60	0.91
	DSL	-0.78	1.00	-0.92	0.71	-0.93
	MCWD	0.80	-0.92	1.00	-0.82	0.86
	S	-0.60	0.71	-0.82	1.00	-0.64
	MAR	0.91	-0.93	0.86	-0.64	1.00
Extreme climatic affiliations:						
		AI	DSL	MCWD	S	MAR
	AI	1.00	-0.90	0.89	-0.71	0.95
	DSL	-0.90	1.00	0.80	0.68	-0.95
	MCWD	0.89	-0.80	1.00	-0.74	0.90
	S	-0.71	0.68	-0.74	1.00	-0.72
	MAR	0.95	-0.95	0.90	-0.72	1.00
Trait sampling climate:						
		AI	DSL	MCWD	S	MAR
	AI	1.00	-0.87	0.79	-0.58	0.94
	DSL	-0.87	1.00	-0.84	0.61	-0.93
	MCWD	0.79	-0.84	1.00	-0.79	0.82
	S	-0.58	0.61	-0.79	1.00	-0.56
	MAR	0.94	-0.93	0.82	-0.56	1.00

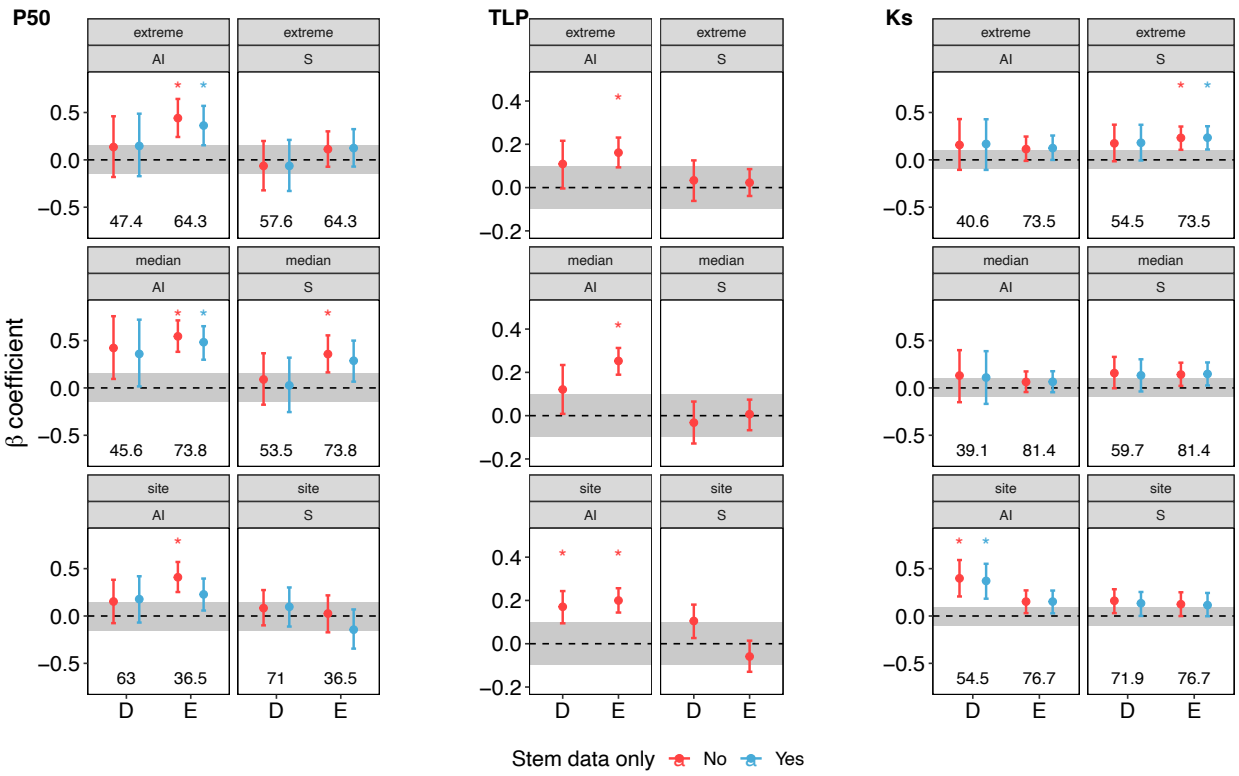

Fig. S1. Regression coefficient (β) values on the effect of aridity index (AI) and rainfall seasonality index (S) on three plant hydraulic traits: stem-specific hydraulic conductivity (KS), leaf water potential at turgor loss point (TLP), and the water potential at 50% loss of conductivity or 50 % accumulation of embolism events in the xylem (P50), obtained by fitting two Bayesian multilevel models: one using data from all observations and one using observations coming from stem data only. For each dataset, we fitted three models: using the extreme climatic affiliation values (extreme), using the median climatic affiliations values (median), and using the climatic values obtained from the trait sampling localities (site). Each point represents the median with its associated 95% high-density credible interval (HDI) for deciduous (D) and evergreen (E) plant species. The shaded gray band represents the region of practical equivalence based on the variability of the response variable in question as [-0.1*sd_Y, 0.1*sd_Y], The asterisks indicate whether 99% of the MCMC distribution falls outside the ROPE, which suggests strong evidence that the climatic predictor affects trait variation. Numbers represent the percentual overlap in the β posterior distributions among datasets.

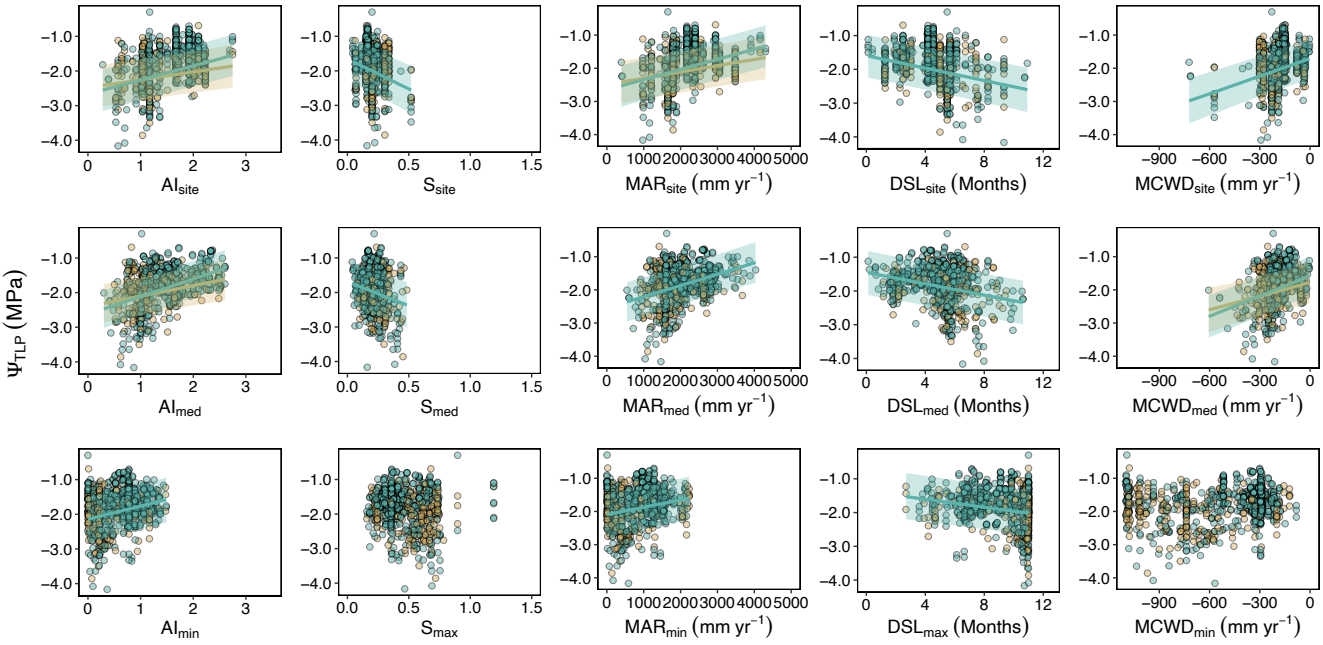

Fig. S2. Scatter plots showing the univariate effects of aridity index (AI), rainfall seasonality (S), mean annual rainfall (MAR), dry season length (DSL), and maximum climatic water deficit (MCWD) on the water potential at leaf turgor loss (Ψ_{TLP}) for evergreen (green) and drought-deciduous (yellow) tropical plants. Regression coefficients (β) were obtained by fitting independent phylogenetic Bayesian multilevel linear models using as climatic predictors the median climatic affiliation values (AI_{med}, S_{med}, MAR_{med}, DSL_{med}, $MCWD_{med}$), the extreme climatic affiliation values (AI_{min}, S_{max}, MAR_{min}, DSL_{max}, $MCWD_{min}$), and the trait sampling localities climate (AI_{site}, S_{site}, MAR_{site}, DSL_{site}, $MCWD_{site}$). Regression lines and their associated 95% high-density credible intervals indicate strong evidence ($\beta \neq 0$) of a given climatic predictor's effect on Ψ_{TLP}.

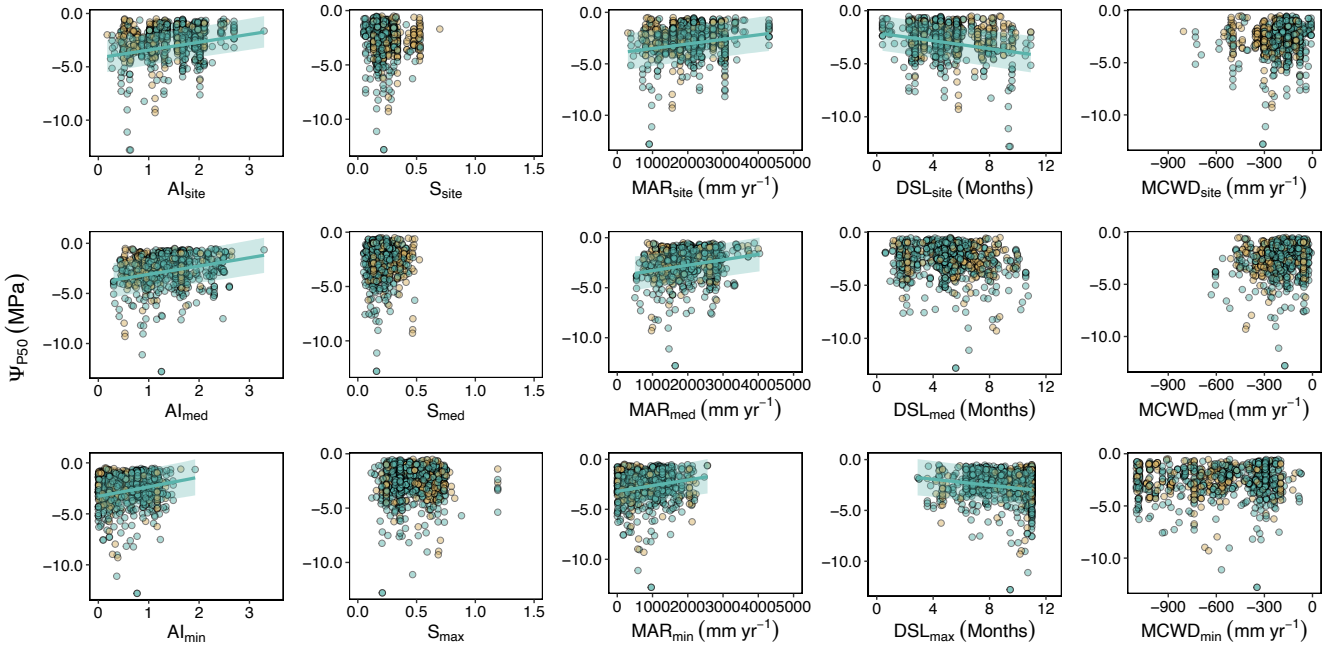

Fig. S3. Scatter plots showing the univariate effects of aridity index (AI), rainfall seasonality (S), mean annual rainfall (MAR), dry season length (DSL), and maximum climatic water deficit (MCWD) on the water potential at 50% loss of conductivity or 50 % accumulation of embolism events in the xylem (Ψ_{P50}) for evergreen (green) and drought-deciduous (yellow) tropical plants. Regression coefficients (β) were obtained by fitting independent phylogenetic Bayesian multilevel linear models using as climatic predictors the median climatic affiliation values (AI_{med}, S_{med}, MAR_{med}, DSL_{med}, $MCWD_{med}$), the extreme climatic affiliation values (AI_{min}, S_{max}, MAR_{min}, DSL_{max}, $MCWD_{min}$), and the trait sampling localities climate (AI_{site}, S_{site}, MAR_{site}, DSL_{site}, $MCWD_{site}$). Regression lines and their associated 95% high-density credible intervals indicate strong evidence ($\beta \neq 0$) of a given climatic predictor's effect on Ψ_{P50}.

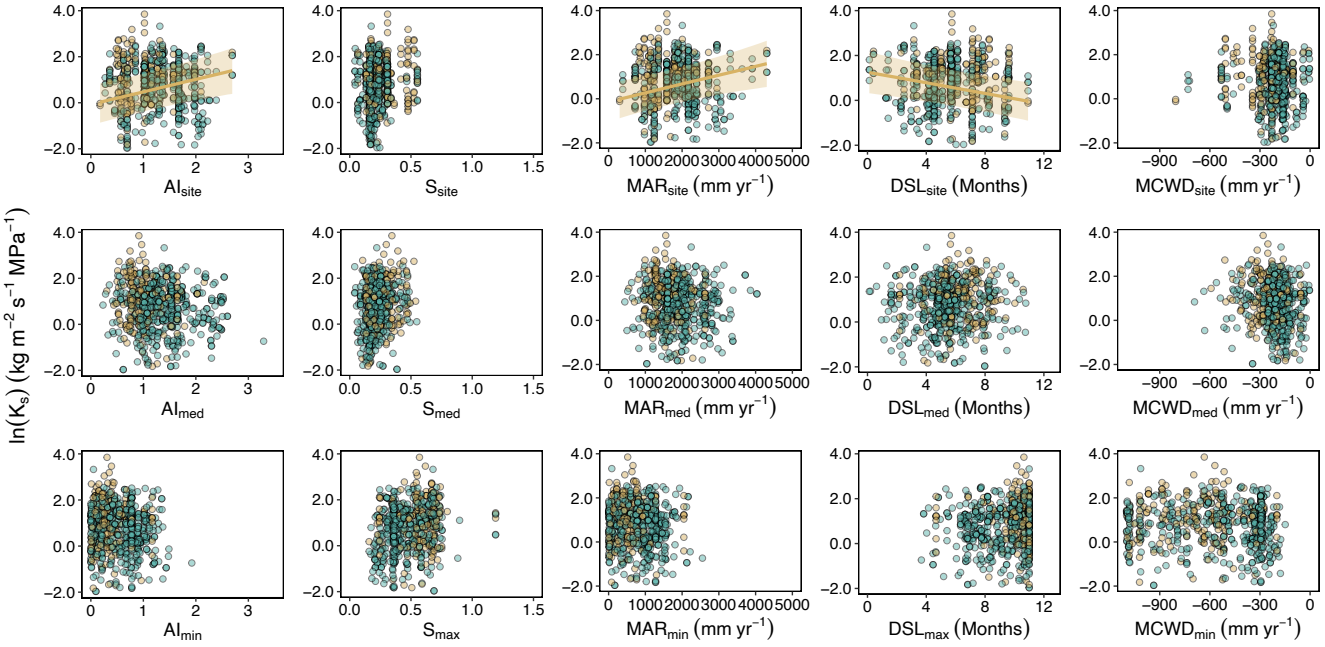

Fig. S4. Scatter plots showing the univariate effects of aridity index (AI), rainfall seasonality (S), mean annual rainfall (MAR), dry season length (DSL), and maximum climatic water deficit (MCWD) on xylem-specific hydraulic conductivity (K_S) for evergreen (green) and drought-deciduous (yellow) tropical plants. Regression coefficients (β) were obtained by fitting independent phylogenetic Bayesian multilevel linear models using as climatic predictors the median climatic affiliation values (AI_{med}, S_{med}, MAR_{med}, DSL_{med}, $MCWD_{med}$), the extreme climatic affiliation values (AI_{min}, S_{max}, MAR_{min}, DSL_{max}, $MCWD_{min}$), and the trait sampling localities climate (AI_{site}, S_{site}, MAR_{site}, DSL_{site}, $MCWD_{site}$). Regression lines and their associated 95% high-density credible intervals indicate strong evidence ($\beta \neq 0$) of a given climatic predictor's effect on K_S.

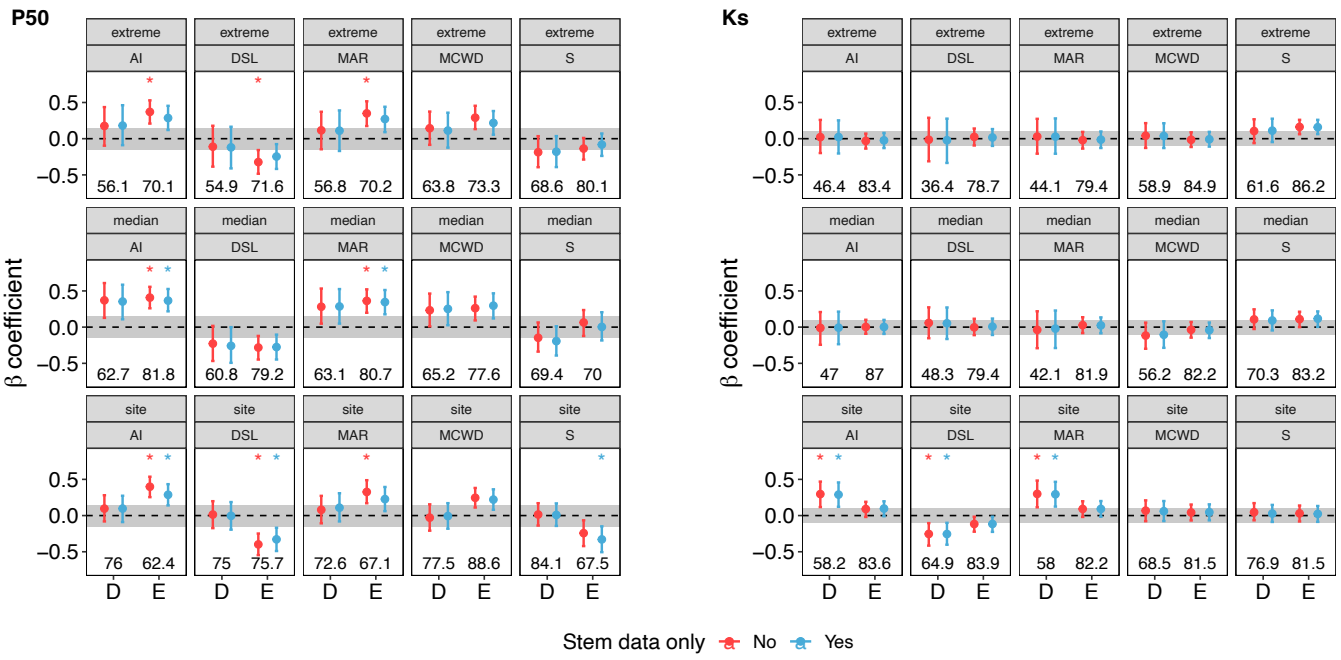

Fig. S5. Regression coefficient (β) values from univariate Bayesian multilevel models of the effect of aridity index (AI), dry season length (DSL), mean annual rainfall (MAR), maximum climatic water deficit (MCWD), and rainfall seasonality index (S) on two plant hydraulic traits: stem-specific hydraulic conductivity (KS) and the water potential at 50% loss of conductivity or 50 % accumulation of embolism events in the xylem (P50). For each climatic predictor, we show coefficients from two models: one using data from all observations and one using observations coming from stem data only. For each dataset, we fitted three models: using the extreme climatic affiliation values (extreme), using the median climatic affiliations values (median), and using the climatic values obtained from the trait sampling localities (site). Each point represents the median with its associated 95% high-density credible interval (HDI) for deciduous (D) and evergreen (E) plant species. The shaded gray band represents the region of practical equivalence based on the variability of the response variable in question as [-0.1*sd_Y, 0.1*sd_Y], The asterisks indicate whether 99% of the MCMC distribution falls outside the ROPE, which suggests strong evidence that the climatic predictor affects trait variation. Numbers represent the percentual overlap in the β posterior distributions among datasets.

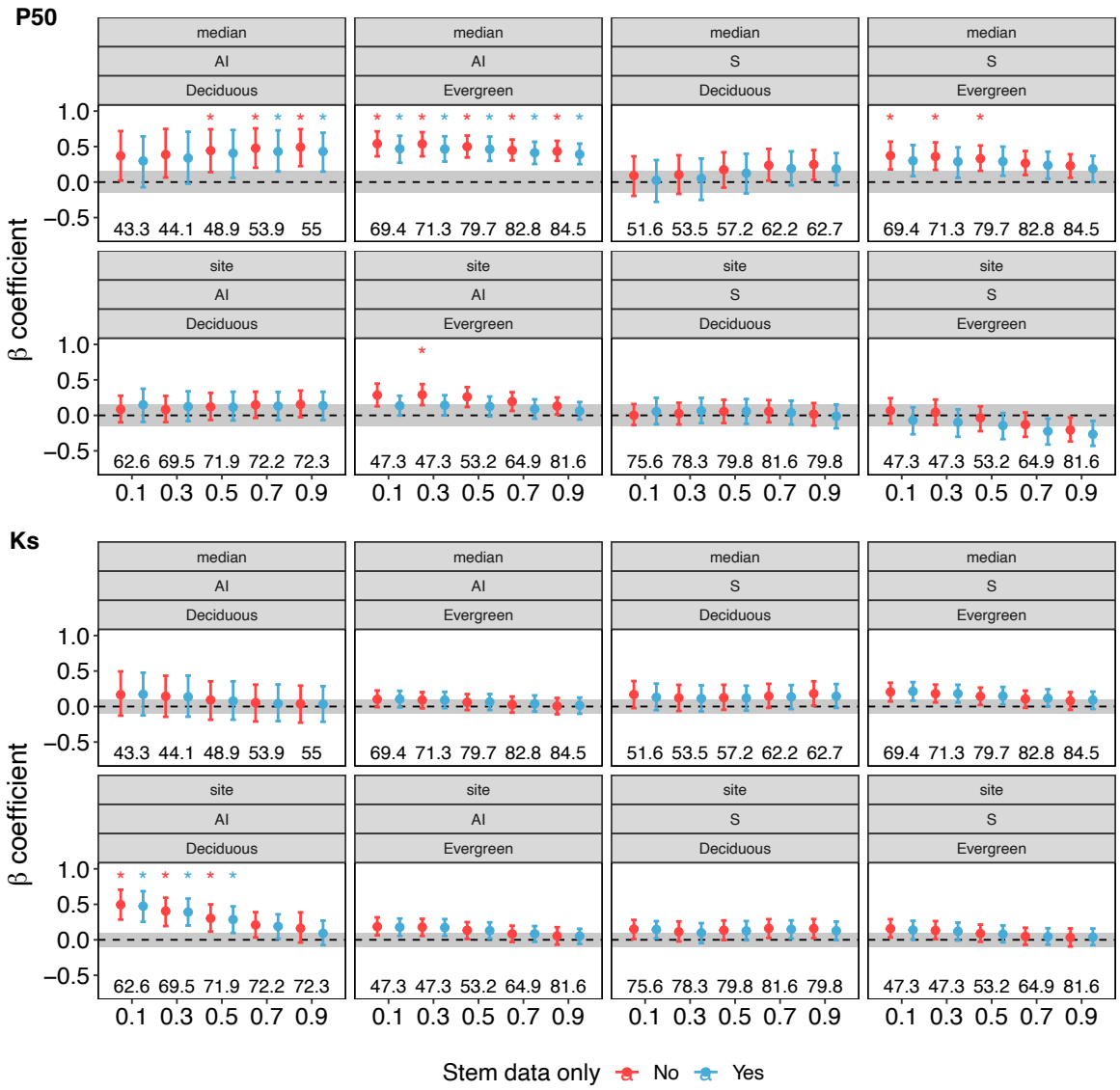

Fig. S6. Quantile regression coefficient (β) values from Bayesian multilevel models on the effect of aridity index (AI), and rainfall seasonality index (S) on two plant hydraulic traits: stem-specific hydraulic conductivity (KS) and the water potential at 50% loss of conductivity or 50 % accumulation of embolism events in the xylem (P50). For each climatic predictor, we show coefficients from two models: one using data from all observations and one using observations coming from stem data only. For each dataset, we fitted two models: using the median climatic affiliations values (median), and using the climatic values obtained from the trait sampling localities (site). Each point represents the median with its associated 95% high-density credible interval (HDI) for deciduous and evergreen plant species. The shaded gray band represents the region of practical equivalence based on the variability of the response variable in question as [-0.1*sd_Y, 0.1*sd_Y], The asterisks indicate whether 99% of the MCMC distribution falls outside the ROPE, which suggests strong evidence that the climatic predictor affects trait variation. Numbers represent the percentual overlap in the β posterior distributions among datasets.

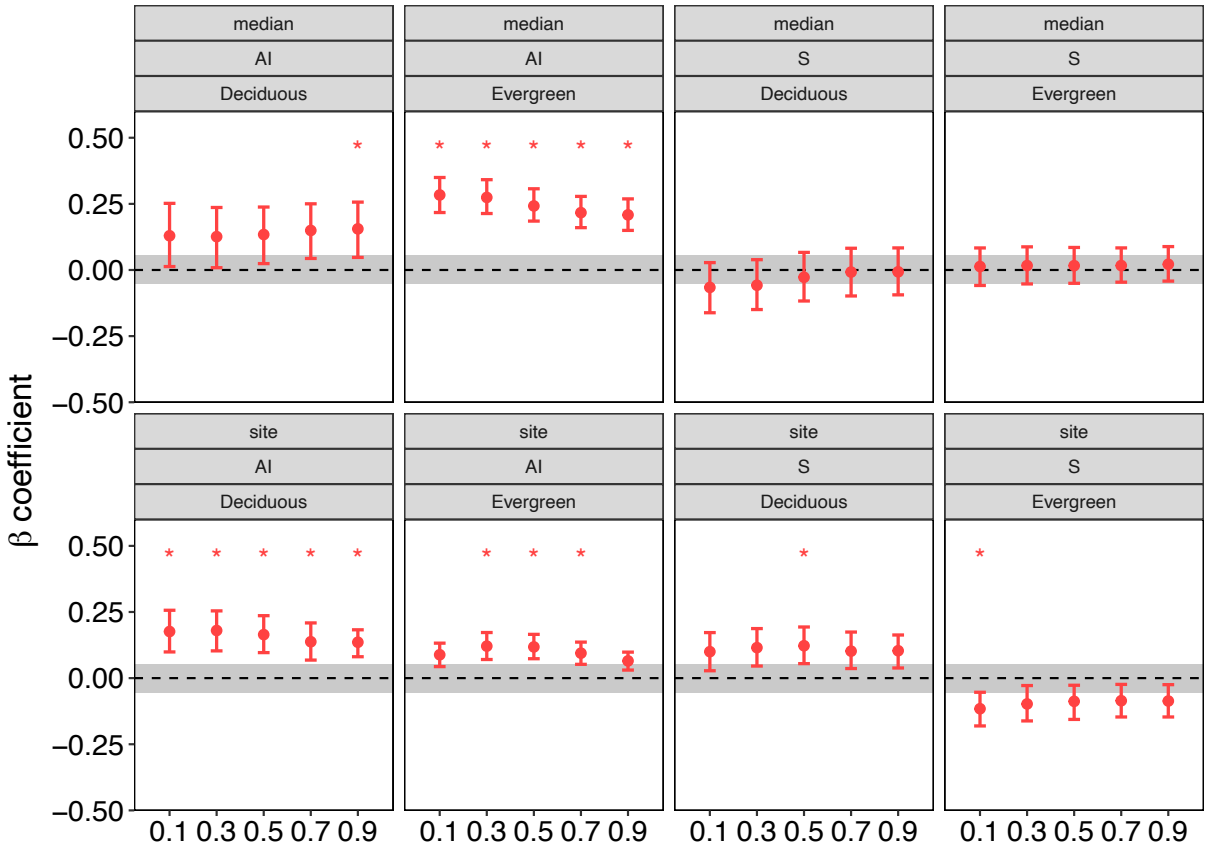

Fig. S7. Quantile regression coefficient (β) values from Bayesian multilevel models on the effect of aridity index (AI), and rainfall seasonality index (S) on the water potential at leaf turgor loss point (Ψ_{TLP}). We fitted two models: using the median climatic affiliations values (median), and using the climatic values obtained from the trait sampling localities (site). Each point represents the median with its associated 95% high-density credible interval (HDI) for deciduous and evergreen plant species. The shaded gray band represents the region of practical equivalence based on the variability of the response variable in question as [-0.1*sd_Y, 0.1*sd_Y], The asterisks indicate whether 99% of the MCMC distribution falls outside the ROPE, which suggests strong evidence that the climatic predictor affects trait variation.

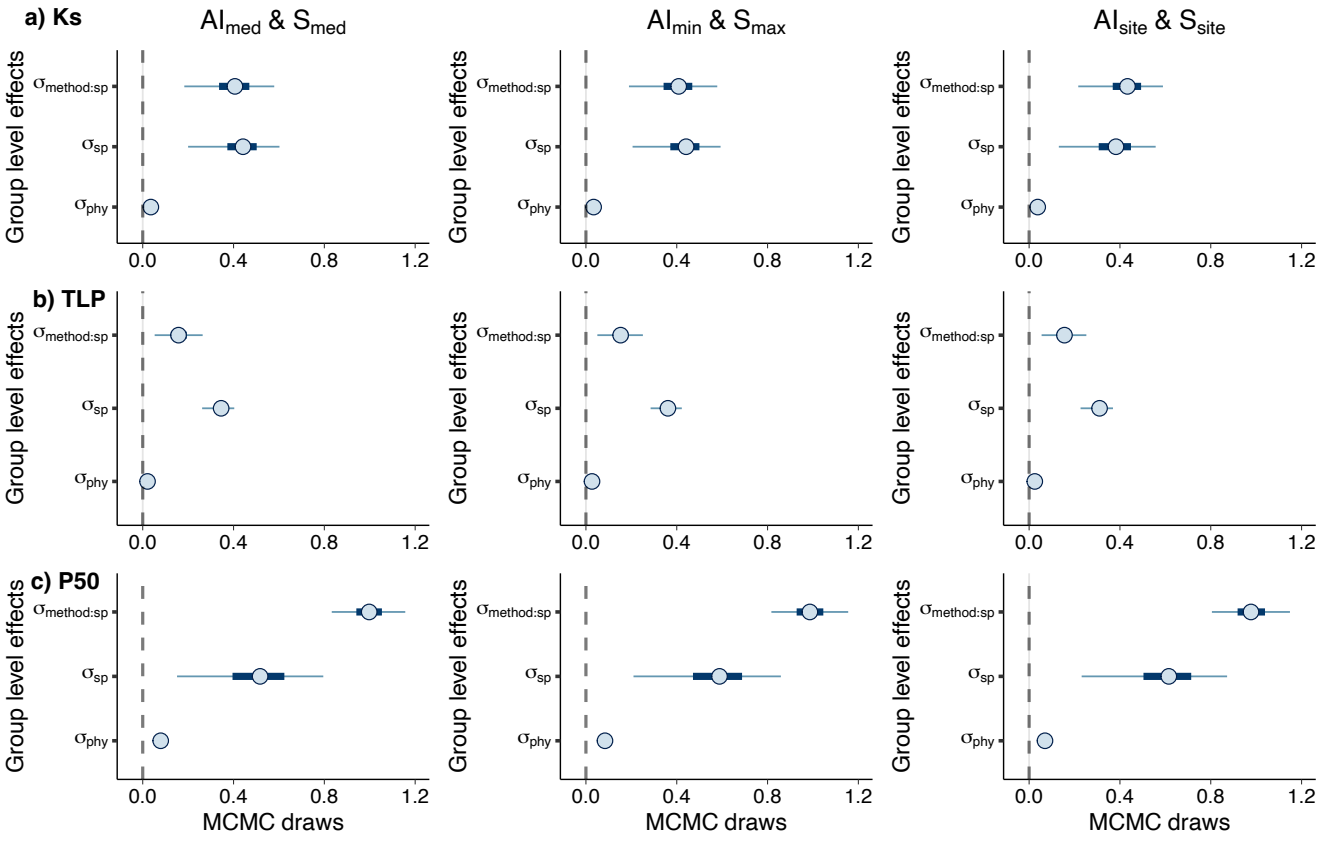

Fig. S8. Group level effects on model variance for the different levels method within species ($\sigma_{method:sp}$), species associated uncertainty (σ_{sp}), and species phylogenetic relatedness (σ_{phy}). The circles represent the median estimate, and the error bars represent the 50% (thick) and 95% (thin) credible intervals.

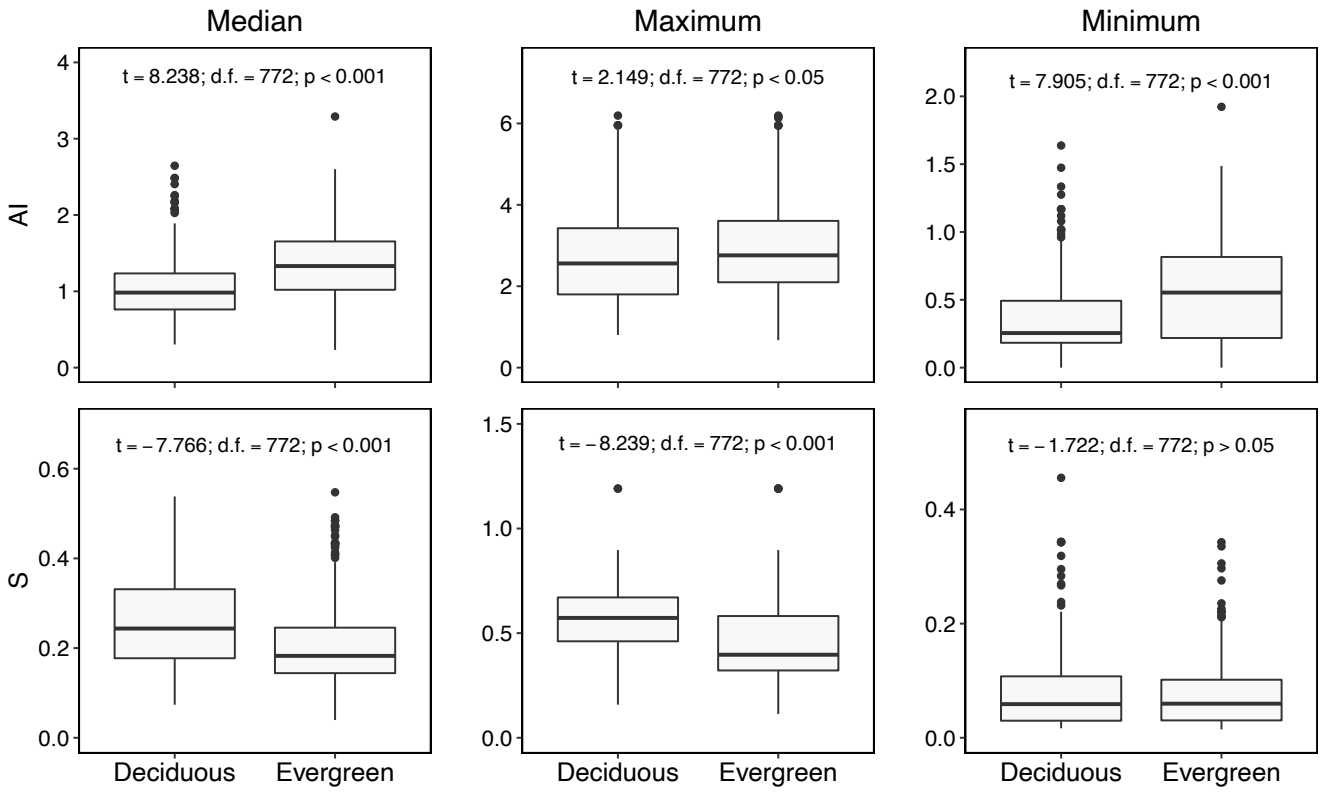

Fig. S9. Boxplots of AI and S values as obtained from species BIEN-derived occurrence records for evergreen and drought-deciduous plant species. Each panel represents the climatic affiliations using the median, maximum, and minimum. Statistical results from a Student t-test comparing values among evergreen and drought-deciduous species. The horizontal line represents the median, the box is defined by the 25th and 75th percentiles, and the whiskers are the maximum values.

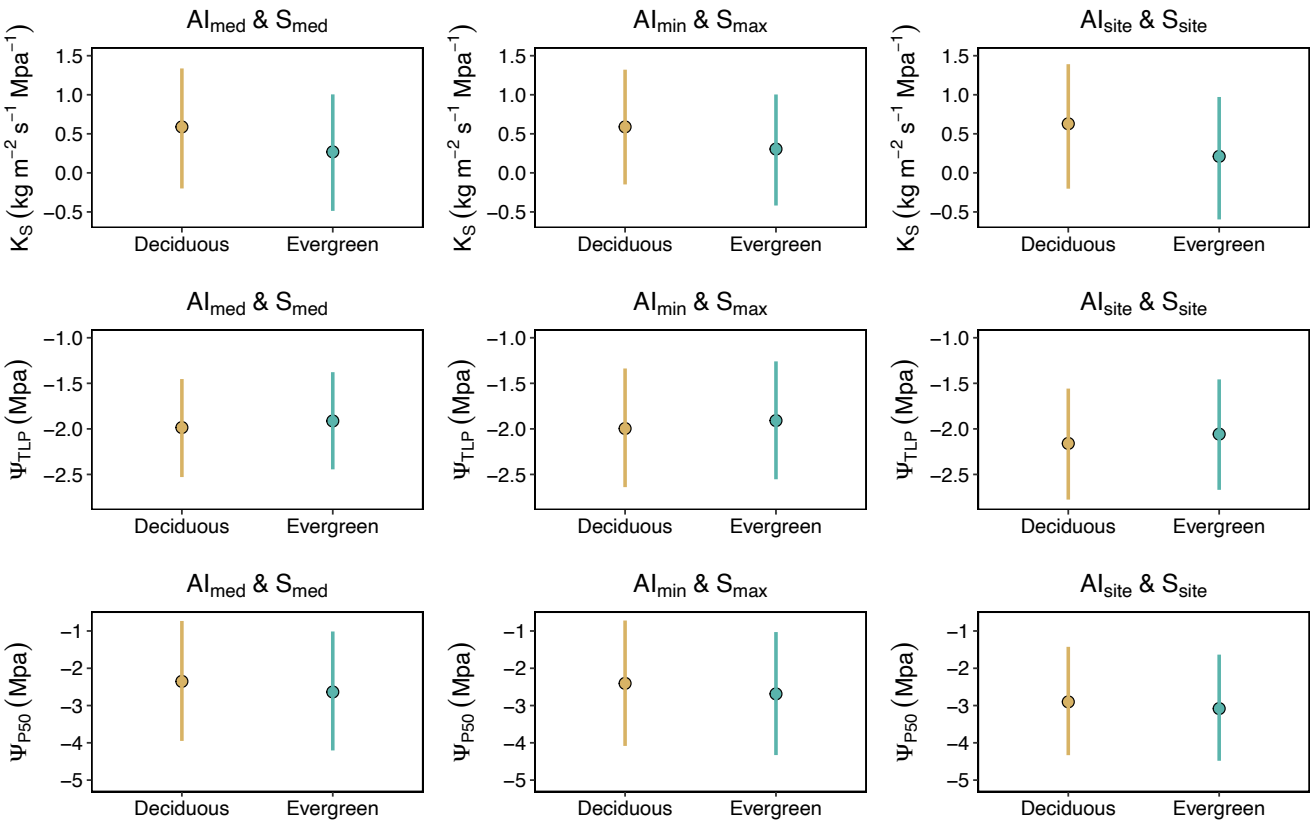

Fig. S10. Posterior median estimates with their associated 95% high-density credible interval of plant hydraulic trait values for drought-deciduous and evergreen pan-tropical plants. Panels depict values for xylem specific hydraulic conductivity (K_S), the water potential at leaf turgor loss (Ψ_{TLP}), and the water potential at 50 % K_S loss or 50 % accumulation of embolism events in the xylem (Ψ_{P50}). Each panel represents a model with the linear combination of climate predictors using species' median climatic affiliation values (AI_{med} and S_{med}), the values linked to the driest and more seasonal environment where the species occurs (AI_{min} and S_{max}), and the climatic values obtained from the trait sampling localities (AI_{site} and S_{site}).

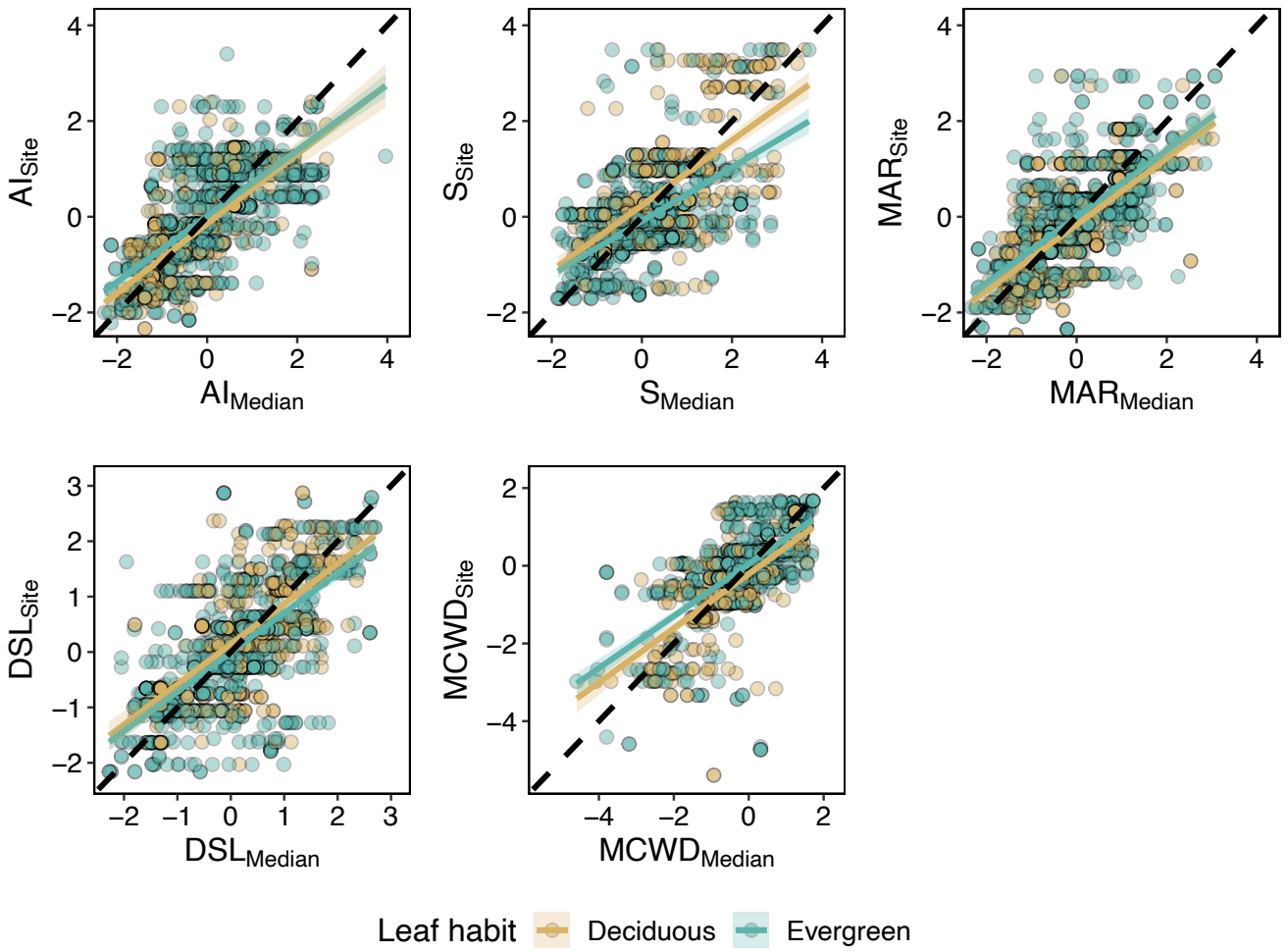

Fig. S11. Sampling site climate as a function of the species' climatic affiliation for the aridity index (AI), the seasonality index (S), mean annual rainfall (MAR), dry season length (DSL), and maximum climatic water deficit (MCWD). Each dot represents an observation of any of the three hydraulic traits in this study at a given sampling site. Straight lines and uncertainties represent the mean response and the 95% high-density interval from a multilevel Bayesian model with species as a random intercept, while the dashed line is the 1:1 relationship. This data shows that in most cases, species were sampled in either wetter or drier regions, less seasonal or more seasonal than their median climatic affiliation.

Notes S1. Reconciliation of species nomenclature conflicts.

We reconciled nomenclature conflicts with the Iplantcollaborative database (http://tnrs.iplantcollaborative.org/TNRSapp.html, accessed June 15th, 2020). The database scored the species name from 0 to 1. When the scores were below 1, names were checked both in the Tropicos (http://www.tropicos.org, accessed July 23rd, 2020) and The Plant List (http://www.theplantlist.org/, accessed July 23rd, 2020) databases. When we encountered discrepancies among databases, the names used in Tropicos were preferred. In case a name was not found in either The Plant List or the Tropicos databases, the whole genus was inspected to find similar names. When two accepted names were valid for a species, we refer to the local botanical authorities in the country where trait data collection took place.

Notes S2. Phylogenetic Bayesian multilevel model to explain plant hydraulic traits variation as a function of aridity and seasonality.

We fitted three intependendent models for each plant hydraulic trait (y), in which we assumed trait variation of the i-th observation follows a normal distribution with a mean (μ) and error (σ_e) that follows a t distribution. Therefore, trait μ is assumed to be the sum of the linear combination of the effects (β) by the climate predictors (AI and S) and leaf habit (LH). In these models, we assigned species-specific intercepts (α_{sp}) and another species-specific intercept associated with the species phylogeny. The residual variation of α_{sp} (σ_{sp}) follows a gamma distribution and α_{phy} assumes that residual trait variation (σ_{phy}) is correlated as indicated by a phylogenetic distance matrix (D). By having two independent intercepts associated with species (α_{sp} and α_{phy}), we assumed that trait variation at the species level is not explained by species phylogenetic relatedness and can be explained by multiple sources not considered in this model (*e.g.*, within-species differences). We used the same model for fitting the quantile regression analysis, but we changed the associated distribution of the response variable from normal to following a Laplace distribution. This change was done in order to account for unequal variation across quantiles in the response of plant hydraulic traits to the climatic predictors. In all models, the posterior distributions were obtained by sampling using a Hamiltonian Monte-Carlo algorithm over four Markov-chains Monte-Carlo (MCMC) with 15000 iterations and a burn-in period of 3000 iterations, as follows.

Likelihood:

$$y_i \sim N(\mu_i, \sigma_e)$$

$$\mu_i = \alpha + \alpha_{sp[i]} + \alpha_{phy[i]} + \beta_1 AI_i + \beta_2 S_i + \beta_3 LH_i + \beta_4 AI_i : LH_i + \beta_5 S_i : LH_i$$

Priors:

$$\alpha_{sp[i]} \sim N(0, \sigma_{sp})$$

$$\sigma_{sp} \sim G(2, 0.2)$$

$$\alpha_{phy[i]} \sim N\left(0, \sigma_{phy}\right)$$

$$\sigma_{phy} \sim \begin{bmatrix} 0 & & & \\ D_{sp_1 - sp_2} & 0 & & \\ \vdots & \cdots & \ddots & \\ D_{sp_1 - sp_n} & \cdots & \cdots & 0 \end{bmatrix}$$

$$\beta_1, \beta_2, \beta_3, \beta_4 \textit{ and } \beta_5 \sim N(0, \sigma_e)$$

$$\alpha \sim N(0, \sigma_e)$$

$$\sigma_e \sim t(4, 0, 5)$$